

Variational wavefunction study of the triangular lattice supersolid

Arnab Sen¹, Prasenjit Dutt¹, Kedar Damle^{1,2}, and R. Moessner^{3,4}

¹*Department of Theoretical Physics, Tata Institute of Fundamental Research, Mumbai 400005, India*

²*Physics Department, Indian Institute of Technology Bombay, Mumbai 400076, India*

³*Rudolf Peierls Centre for Theoretical Physics, Oxford University, Oxford OX1 3NP, UK*

⁴*Max-Planck-Institut für Physik komplexer Systeme, 01189 Dresden, Germany*

(Dated: November 8, 2018)

We present a variational wavefunction which explains the behaviour of the supersolid state formed by hard-core bosons on the triangular lattice. The wavefunction is a linear superposition of *only and all* configurations minimising the repulsion between the bosons (which it thus implements as a hard constraint). Its properties can be evaluated exactly—in particular, the variational minimisation of the energy yields (i) the surprising and initially controversial spontaneous density deviation from half-filling (ii) a quantitatively accurate estimate of the corresponding density wave (solid) order parameter.

PACS numbers: 75.10.Jm 05.30.Jp 71.27.+a

There has been sustained interest in using ultracold atoms confined in optical lattice potentials to realize strongly-correlated systems of interest to condensed matter physics [1]. The recently discussed possibility that Helium has a supersolid phase[2] leads, in this context, to a natural question: Can the lattice analog of this, namely a superfluid phase that simultaneously breaks lattice translation symmetry, be seen in such optical lattice experiments?

Although other examples are known [2], perhaps the best candidate for such a lattice supersolid persisting over a wide range of parameters (such as chemical potential and interaction energy) is that observed numerically in several recent Quantum Monte-Carlo (QMC) studies of a two-dimensional system of strongly interacting bosons in a triangular lattice potential [3, 4, 5], and confirmed in subsequent follow-up work [6]. Following earlier work [7], these QMC studies considered the model Hamiltonian:

$$H = -t \sum_{\langle ij \rangle} (b_i^\dagger b_j + b_j^\dagger b_i) + V \sum_{\langle ij \rangle} (n_i - 1/2)(n_j - 1/2) \quad (1)$$

where b_i^\dagger (b_i) is the boson creation (annihilation) operator, t represents the strength of the boson hopping amplitude, V is the strength of the nearest neighbour repulsion, and the bosons are restricted to be in the hard-core limit ($n_i = 0, 1$) by a strong onsite repulsive term not written down explicitly (here, we have only displayed the Hamiltonian for the value of the chemical potential μ at which the system has particle-hole symmetry). Strikingly, in this particle-hole symmetric, hard-core case, an *extended* supersolid state was observed numerically for *all* $V/t \geq 8.9$, and seen to possess both a non-zero superfluid stiffness, and density wave (‘solid’) order at the three sublattice ($\sqrt{3} \times \sqrt{3}$ ordering) wavevector \vec{Q} (the state is stable to changes in μ as well).

There are two other genuinely surprisingly features of this phase. The first [4] concerns the nature of the solid order. Plausible mean-field theory arguments [5] predict

that the density wave order in the supersolid at $\mu = 0$ should involve a ‘(+ − 0)’ type three sub-lattice pattern of density with $\rho_a = 1/2$, $\rho_b = 1/2 + \delta$, $\rho_c = 1/2 - \delta$, while in reality the system prefers a different ‘(+ − −)’ pattern with the same ordering wavevector: $\rho_a = 1/2 + \delta_1$, $\rho_b = \rho_c = 1/2 - \delta_2$, with $\delta_{1,2} > 0$ (Fig 1). General symmetry arguments [4, 5] predict that the *total* density of the system should also exhibit a spontaneous deviation from half-filling in a ‘(+ − −)’ state. The second surprise is that although there is such a deviation, it is *extremely small* in ‘natural’ units (i.e compared to the strength of the density wave order itself), and therefore extremely difficult to see numerically [4, 5].

In order to understand this large V/t supersolid phase in the hardcore limit, it is necessary to take into account this strong repulsion as a hard constraint. Here we consider an analytically tractable variational wavefunction that takes into account this hard constraint from the start, and uses a variational parameter to tune the amplitudes of different minimum repulsion energy configurations. The energetically optimal wavefunction accounts for both qualitative (‘(+ − −)’ order) and quantitative (size of the order parameter) aspects of the supersolid phase in the limit of strong nearest neighbour repulsion. Our treatment thus represents a remarkable instance in which a non-trivial constraint *on the lattice scale* imposed by a dominant term in the Hamiltonian can be taken into account in an exact manner in a variational calculation—for instance, the celebrated problem of accounting for the single-occupancy constraint imposed (by strong coulomb repulsion) on holes in the *Cu-O* planes of high- T_c superconductors has resisted analytical treatment thus far.

Our starting point is the observation that the supersolid ground state at large V/t must have a wavefunction that lies entirely in the subspace of minimum interaction energy configurations. More precisely, in the classical ($t = 0$) limit, the ground states are diagonal in the particle-number basis, and form an extensively degener-

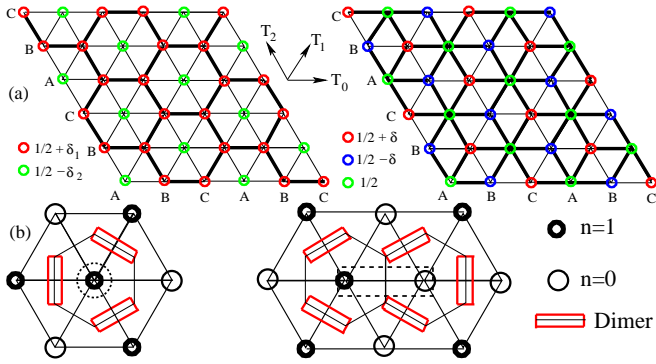


FIG. 1: (color online). a) The two possible supersolid states at the three-sublattice wavevector \vec{Q} . Dark (light) links represent higher (lower) bond kinetic energy, and sites are color coded to reflect mean density. b) Flippable single and double hexagons in the dimer representation, and the corresponding local density configuration.

ate set of states corresponding to all minimum repulsion energy configurations of particles. To leading order in t/V , the slow dynamics induced by the kinetic energy term then leads to an effective Hamiltonian \mathcal{H} acting in within this manifold of states:

$$\mathcal{H}_{eff} = -t \sum_{\langle ij \rangle} \mathcal{P}_g (b_i^\dagger b_j + b_j^\dagger b_i) \mathcal{P}_g \quad (2)$$

where \mathcal{P}_g is the projection operator to the minimum repulsion energy subspace.

As H maps to a system of $S = 1/2$ spins ($S_i^z = n_i - 1/2$ where n_i is the boson number at site i) with *frustrated* antiferromagnetic exchange $J^z = V$ between the z components of neighbouring spins, ferromagnetic exchange $J_\perp = 2t$ between their x and y components, and magnetic field $B_z \propto \mu$, the ground states in this $t = 0$ limit may be identified with minimally frustrated states of the classical Ising antiferromagnet on the triangular lattice [8]. As is well-known, these may be conveniently characterized in terms of dimer coverings of the dual honeycomb lattice (with a dimer placed on the dual link perpendicular to every frustrated bond of a given spin configuration). In this language, \mathcal{H}_{eff} is simply a quantum dimer model with a *ring-exchange term* that acts on each pair of adjacent hexagons on the dual honeycomb lattice (corresponding to each bond $\langle ij \rangle$ of the triangular lattice):

$$\mathcal{H}_{eff} = -t \sum_{\langle ij \rangle} (|\infty_{\langle ij \rangle}\rangle \langle \infty_{\langle ij \rangle}| + h.c.) \quad (3)$$

Thus, the supersolid behaviour at large V/t should be understood in terms of the ground state of this quantum dimer model. As was noted in earlier literature [4, 5], a trial state obtained from an equal amplitude superposition of *all* minimum interaction energy configurations (which maps, apart from a global particle-hole transformation, to a uniform superposition of dimer covers of the

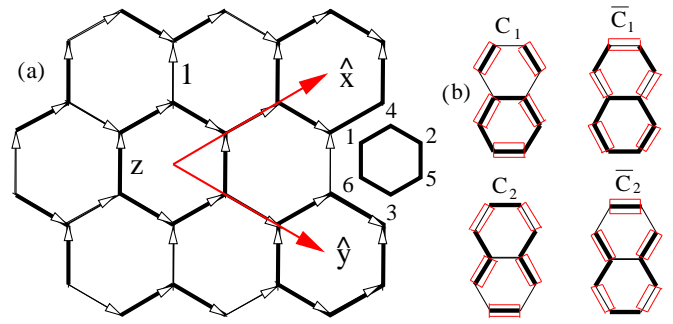


FIG. 2: (color online). a) Dimer ensemble with a three-sublattice pattern of fugacities which breaks lattice translation symmetry at wavevector \vec{Q} . b) The two types of flippable double-hexagons, with two flippable configurations each—note that light (dark) links correspond to fugacities 1 (z).

honeycomb lattice) already provides a substantial kinetic energy gain, while minimizing the inter-particle repulsion by construction.

Since $\langle \Psi_0 | b_i^\dagger | \Psi_0 \rangle$ is clearly proportional to the *non-zero* probability that hexagon i is *flippable* in the classical dimer model, this trial state immediately provides a rationale for the persistence of off-diagonal long-range order and superfluidity in the large V/t limit. On the other hand, this trial state is unable to fully account for the density wave order of the true supersolid state, as density correlators in $|\Psi_0\rangle$ map on to spin correlations of the $T = 0$ classical Ising antiferromagnet on the triangular lattice which does not support genuine long-range order [8], but instead displays power-law order at the three-sublattice wavevector [9].

Here, we focus instead on a variational state obtained from a dimer model with two types of links, with different dimer fugacities 1 and $z \geq 0$, defined on the honeycomb lattice in a pattern (Fig 2) which breaks lattice symmetry at wavevector \vec{Q} for all $z \neq 1$:

$$|\Psi_{var}(z)\rangle = \sum_{C_d} \sqrt{P_{C_d}(z)/2} (|n_+(C_d)\rangle + |n_-(C_d)\rangle) \quad (4)$$

where $P_{C_d}(z)$ is the probability of a dimer configuration C_d in this dimer model, and the two particle-hole conjugate configurations $|n_\pm(C_d)\rangle$ corresponding to C_d occur with the same amplitude in this nodeless wavefunction (this follows from the Perron-Frobenius theorem, as was noted earlier in a different context[10]).

Clearly, $|\Psi(z)\rangle$ is characterized by three-sublattice density wave order of the $(+ - -)$ type (see Fig 1) for $z < 1$ while for $z > 1$, it displays density wave order of the $(+ - 0)$ type. Furthermore, as the state is constructed from a coherent superposition of Fock states with a considerably wide distribution of average density, $|\Psi(z)\rangle$ is expected to also possess off-diagonal long range order associated with superfluidity, at least for z close to $z = 1$.

In order to perform an unbiased variational study, we need to locate minima of the varia-

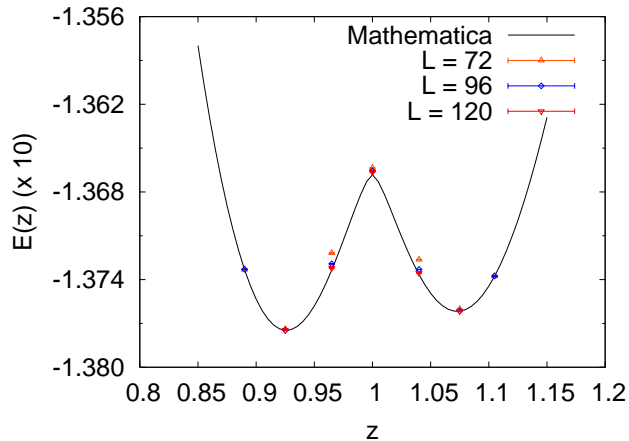


FIG. 3: (color online). Variational energy per site in units of $2t$ as a function of z .

tional estimate of energy per site (in units of $2t$): $E(z) = \langle \Psi_{var}(z) | \mathcal{H}_{eff} | \Psi_{var}(z) \rangle / 2tL^2$. To calculate $E(z)$, we note that $\langle \Psi_{var}(z) | \mathcal{P}_g b_i^\dagger b_j \mathcal{P}_g | \Psi_{var}(z) \rangle = \sqrt{P(\mathfrak{C}_{\langle ij \rangle}) P(\mathfrak{C}_{\langle ij \rangle})}$, where $P(\mathfrak{C}_{\langle ij \rangle})$ and $P(\mathfrak{C}_{\langle ij \rangle})$ are the probabilities that the double hexagon $\langle ij \rangle$ is in the *flippable* configurations depicted in their respective arguments. This allows us to write

$$E(z) = - \left(2\sqrt{P(1\mathcal{C})P(1\bar{\mathcal{C}})} + \sqrt{P(2\mathcal{C})P(2\bar{\mathcal{C}})} \right) \quad (5)$$

where $P(1\mathcal{C})$ and $P(1\bar{\mathcal{C}})$ ($P(2\mathcal{C})$ and $P(2\bar{\mathcal{C}})$) are the respective probabilities that type 1 (type 2) double-hexagons are in flippable configurations \mathcal{C} and $\bar{\mathcal{C}}$ (see Fig 2). Thus, the variational energy is lowered if the expected number of *flippable double-hexagons* is large. Since the number of flippable double hexagons must decrease rapidly to zero in the $z \rightarrow 0$ as well as the $z \rightarrow \infty$ limit as the dimers freeze into a perfect columnar or plaquette state in these limits, it is immediately clear that one or more variational minima of $E(z)$ must occur at or in the vicinity of the translationally invariant point $z = 1$.

Calculation of the probabilities P is greatly facilitated by the well-known formulation of dimer models on planar graphs in terms of Grassmann variables [11, 12, 13]: For the case at hand, this can be obtained by using the ‘arrow convention’ displayed in Fig 2 to define an antisymmetric matrix M , with $M_{ij} = +\mu_{\langle ij \rangle}$ (where the fugacity associated with link $\langle ij \rangle$) if an arrow points from point i to j and $M_{ij} = -\mu_{\langle ij \rangle}$ if the arrow goes from j to i ($M_{ij} = 0$ if i, j are not nearest neighbours, $\mu_{\langle ij \rangle}$ equals z or 1 as shown in Fig 2). The dimer partition function Z is then obtained as $Z = |Pf[M]| = |\int [\mathcal{D}\psi] \exp(S)|$, where Pf denotes the Pfaffian and $S = \sum_{i < j} M_{ij} \psi_i \psi_j$ is the action for Grassmann variables ψ_i defined on sites of the honeycomb lattice.

To proceed further, we represent the honeycomb net

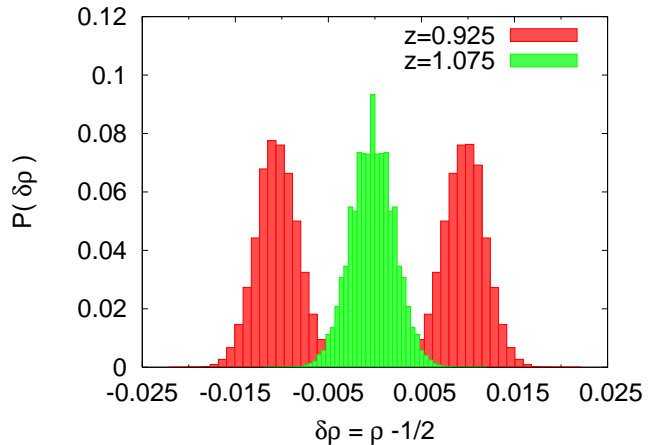


FIG. 4: (color online). Distribution of the total density at the global variational minimum at $z \approx 0.925$, as well as at the competing local minimum at $z \approx 1.07$. Data shown is for $L = 96$.

as an underlying triangular Bravais lattice with Roman letter coordinates (representing centers of those hexagons whose links all have fugacity z) that is decorated by six basis points (corresponding to vertices of such hexagons) labeled by Greek letters (Fig 2), and write the action as $S = \frac{1}{2} \sum_{\vec{x}, \alpha} \sum_{\vec{y}, \beta} M_{\vec{x}, \vec{y}}^{\alpha, \beta} \psi_{\alpha, \vec{x}} \psi_{\beta, \vec{y}}$. Transforming to Fourier space, we obtain $S = \frac{1}{2} \sum_{\vec{k}, \alpha, \beta} \tilde{M}_{\vec{k}}^{\alpha, \beta} \psi_{\alpha, \vec{k}} \psi_{\beta, -\vec{k}}$, with the 6×6 matrix $\tilde{M}_{\vec{k}}^{\alpha, \beta}$ is given as

$$\tilde{M}(\vec{k}) = \begin{pmatrix} \mathbf{0} & \tilde{\mathbf{R}}(\vec{k}) \\ -\tilde{\mathbf{R}}^\dagger(\vec{k}) & \mathbf{0} \end{pmatrix}$$

where $\mathbf{0}$ is the 3×3 null matrix and $\tilde{\mathbf{R}}$ can be written as

$$\tilde{\mathbf{R}}(\vec{k}) = \begin{pmatrix} z & -e^{-ik_y} & -z \\ -z & -z & e^{ik_x} \\ -e^{-ik_x + ik_y} & z & -z \end{pmatrix}$$

Next, we note that this Grassmann formulation provides a simple prescription for the probability that five dimers occupy alternate links $l_1 \dots l_5$ on the perimeter of double hexagon made up of points $i = 1, 2 \dots 10$:

$$P(\{l_1 \dots l_5\}) = \left(\prod_{m=1}^5 \mu_{l_m} \right) \cdot |\langle \psi_1 \psi_2 \psi_3 \dots \psi_{10} \rangle| \quad (6)$$

where μ_{l_m} are the fugacities of the 5 links occupied by dimers. This allows us to write $E(z)$ as

$$E(z) = -2z^{\frac{7}{2}} |\langle \psi_1 \psi_2 \psi_3 \dots \psi_{10} \rangle_1| - z^3 |\langle \psi_1 \psi_2 \psi_3 \dots \psi_{10} \rangle_2| \quad (7)$$

where the subscripts on the 10-point correlators refer to the type of double-hexagon on which they are calculated (see Fig 2).

The 10 point correlators involved in this expression can be computed in the free field action S using Wick's theorem and knowledge of the two point correlators:

$$\langle \psi_{\alpha, \vec{x}} \psi_{\beta, \vec{y}} \rangle = \int \frac{d^2 k}{4\pi^2} \exp(-i\vec{k} \cdot (\vec{x} - \vec{y})) (-\mathbf{M}^{-1}(-\vec{k}))_{\alpha, \beta} (8)$$

where the integration is over the Brillouin zone $k_x, k_y \in (-\pi, \pi]$. As $\langle \psi_i \psi_j \rangle = 0$ if i and j belong to the same sublattice on the honeycomb lattice, one needs to keep track of 'only' $5! = 120$ contractions in evaluating either of the two 10-point correlators. Keeping track of these contractions and performing the required k integrations using MATHEMATICA, we obtain the variational energy $E(z)$ shown in Fig 3. As is clear from this figure, $E(z)$ has two minima, a global minimum at $z \approx 0.9250$, and local minimum at $z \approx 1.0750$ with energy only very slightly higher (by about $\approx 0.047\%$) than its value at the global minimum.

Thus, our variational calculation yields a $(+ - -)$ type three sublattice ordered supersolid state in the large V/t limit, and suggests that the energy of the $(+ - 0)$ supersolid at the same wavevector is only slightly higher than that of the $(+ - -)$ supersolid. In order to obtain an independent verification of this result, we have also used the method of Ref [14] to simulate the corresponding dimer model and numerically calculate $E(z)$ —the results of these calculations are seen to match precisely with the results obtained by Grassmann techniques (Fig 3).

This simulation also allows us to measure directly the solid order parameter $\psi = m_a + m_b e^{2\pi i/3} + m_c e^{4\pi i/3}$, where m_a, m_b, m_c are the number densities on the three sublattices of the triangular lattice. We obtain $|\psi|^2 = 0.03885$ for the global minimum at $z = 0.9250$, which agrees within 10% with the results from QMC [5] extrapolated to $V/t \rightarrow \infty$. (the value in the competing $(+ - 0)$ state is $|\psi|^2 = 0.03697$ at the slightly higher energy local minimum at $z = 1.0750$). In addition, we also measure the histogram of the total density, from which one may calculate the ground state expectation values of all powers of the density in the supersolid state. While the local minimum at slightly higher energy has no spontaneous deviation of density from half-filling, we find that the density histogram at the global minimum shows a characteristic two-peak structure, reflecting a very small ($\sim 2\%$) spontaneous deviation from half-filling characteristic of the $(+ - -)$ supersolid (Fig 4).

To obtain further insight into the smallness of this spontaneous density deviation from half-filling, we note that reducing z slightly from $z = 1$ introduces a field coupled to the Fourier component of the particle-density at wavevector \vec{Q} . The effect of this field can be understood by using the well-known [15] height model formulation of $z = 1$ dimer model in terms of an action $S_h = \kappa \int d^2 x (\nabla h)^2$ for a 'height' field $h(x)$ in terms of which one may write the Fourier component of the particle density at wavevector \vec{Q} as $\rho_{\vec{Q}} \sim \exp(i\pi h/3)$, and

at wavevector 0 as $\rho_{tot} \sim \exp(i\pi h)$.

For $z < 1$ but close to $z = 1$, the response of the density at these two wavevectors can be obtained by calculating the corresponding susceptibilities, and one finds that the response at wavevector \vec{Q} is much larger than at wavevector 0, thereby providing a rationalization for the smallness of this symmetry allowed density deviation (in comparison with the size of the order parameter).

Thus, our variational approach provides a coherent picture of the triangular lattice supersolid at large V/t : Kinetic energy effects are seen to select a $(+ - -)$ supersolid state with a three-sublattice density wave order parameter comparable in magnitude to the mean density itself. In addition, the competing $(+ - 0)$ supersolid is seen to be very close in energy to this variational ground state, consistent with numerical evidence and analytical arguments [16] that the order parameter phase (which distinguishes between these two states) is only weakly pinned in the supersolid state. Furthermore, the spontaneous deviation of the density from $1/2$ is seen to be a very small fraction ($\sim 2\%$) of the mean density, consistent with the surprisingly small value obtained in earlier QMC studies.

Acknowledgements: We thank D. Dhar for very insightful discussions and S. L. Sondhi for collaboration on closely related work. We acknowledge computational resources at TIFR and Oxford and support from DST SR/S2/RJN-25/2006 (KD), the John Fell OUP Research Fund-Oxford-India network in Theoretical Physical Sciences (AS), and a British Council RXP grant (RM).

-
- [1] I. Bloch, J. Dalibard, and W. Zwerger, arXiv:0704.3011 (*to appear in Rev. Mod. Phys.*).
 - [2] http://online.kitp.ucsb.edu/online/smatter_m06
 - [3] S. Wessel and M. Troyer, Phys. Rev. Lett. **95**, 127205 (2005).
 - [4] D. Heidarian and K. Damle, Phys. Rev. Lett. **95**, 127206 (2005).
 - [5] R. Melko *et al.*, Phys. Rev. Lett. **95**, 127207 (2005).
 - [6] M. Bonninsegni and N. Prokof'ev, Phys. Rev. Lett. **95**, 237204 (2005).
 - [7] G. Murthy, D. Arovas, and A. Auerbach, Phys. Rev. B **56**, 3104 (1997).
 - [8] G. H. Wannier, Phys. Rev. **79**, 357 (1950).
 - [9] J. Stephenson, J. Math. Phys. **11**, 413 (1970).
 - [10] R. Moessner and S. L. Sondhi, Phys. Rev. B **63**, 224401 (2001).
 - [11] P. W. Kasteleyn, J. Math. Phys. **4**, 287 (1963).
 - [12] S. Samuel, J. Math. Phys. **21**, 2806 (1980).
 - [13] R. Moessner and S. L. Sondhi, Phys. Rev. B **62**, 14122 (2000).
 - [14] A. W. Sandvik and R. Moessner, Phys. Rev. B **73**, 144504 (2006).
 - [15] B. Nienhuis, H. J. Hilhorst, and H. J. W. Blote, J. Phys. A **17**, 3559 (1984).
 - [16] A. A. Burkov and L. Balents, Phys. Rev. B **72**, 134502 (2005).